Di-electron Widths of the Upsilon(1S,2S,3S) Resonances

J. L. Rosner,[1] N. E. Adam,[2] J. P. Alexander,[2] K. Berkelman,[2] D. G. Cassel,[2] J. E. Duboscq,[2] K. M. Ecklund,[2] R. Ehrlich,[2] L. Fields,[2] R. S. Galik,[2] L. Gibbons,[2] R. Gray,[2] S. W. Gray,[2] D. L. Hartill,[2] B. K. Heltsley,[2] D. Hertz,[2] C. D. Jones,[2] J. Kandaswamy,[2] D. L. Kreinick,[2] V. E. Kuznetsov,[2] H. Mahlke-Krüger,[2] T. O. Meyer,[2] P. U. E. Onyisi,[2] J. R. Patterson,[2] D. Peterson,[2] E. A. Phillips,[2] J. Pivarski,[2] D. Riley,[2] A. Ryd,[2] A. J. Sadoff,[2] H. Schwarthoff,[2] X. Shi,[2] S. Stroiney,[2] W. M. Sun,[2] T. Wilksen,[2] M. Weinberger,[2] S. B. Athar,[3] P. Avery,[3] L. Breva-Newell,[3] R. Patel,[3] V. Potlia,[3] H. Stoeck,[3] J. Yelton,[3] P. Rubin,[4] C. Cawlfield,[5] B. I. Eisenstein,[5] I. Karliner,[5] D. Kim,[5] N. Lowrey,[5] P. Naik,[5] C. Sedlack,[5] M. Selen,[5] E. J. White,[5] J. Wiss,[5] M. R. Shepherd,[6] D. M. Asner,[7] K. W. Edwards,[7] D. Besson,[8] T. K. Pedlar,[9] D. Cronin-Hennessy,[10] K. Y. Gao,[10] D. T. Gong,[10] J. Hietala,[10] Y. Kubota,[10] T. Klein,[10] B. W. Lang,[10] R. Poling,[10] A. W. Scott,[10] A. Smith,[10] S. Dobbs,[11] Z. Metreveli,[11] K. K. Seth,[11] A. Tomaradze,[11] P. Zweber,[11] J. Ernst,[12] K. Arms,[13] H. Severini,[14] S. A. Dytman,[15] W. Love,[15] S. Mehrabyan,[15] V. Savinov,[15] O. Aquines,[16] Z. Li,[16] A. Lopez,[16] H. Mendez,[16] J. Ramirez,[16] X. Bo,[17] G. S. Huang,[17] D. H. Miller,[17] V. Pavlunin,[17] B. Sanghi,[17] I. P. J. Shipsey,[17] G. S. Adams,[18] M. Anderson,[18] J. P. Cummings,[18] I. Danko,[18] J. Napolitano,[18] Q. He,[19] J. Insler,[19] H. Muramatsu,[19] C. S. Park,[19] E. H. Thorndike,[19] T. E. Coan,[20] Y. S. Gao,[20] F. Liu,[20] R. Stroynowski,[20] M. Artuso,[21] S. Blusk,[21] J. Butt,[21] J. Li,[21] N. Menaa,[21] R. Mountain,[21] S. Nisar,[21] K. Randrianarivony,[21] R. Redjimi,[21] R. Sia,[21] T. Skwarnicki,[21] S. Stone,[21] J. C. Wang,[21] K. Zhang,[21] S. E. Csorna,[22] G. Bonvicini,[23] D. Cinabro,[23] M. Dubrovin,[23] A. Lincoln,[23] R. A. Briere,[24] J. Chen,[24] T. Ferguson,[24] G. Tatishvili,[24] H. Vogel,[24] and M. E. Watkins[24]

(CLEO Collaboration)

[1]*Enrico Fermi Institute, University of Chicago, Chicago, Illinois 60637*

[2]*Cornell University, Ithaca, New York 14853*

[3]*University of Florida, Gainesville, Florida 32611*

[4]*George Mason University, Fairfax, Virginia 22030*

[5]*University of Illinois, Urbana-Champaign, Illinois 61801*

[6]*Indiana University, Bloomington, Indiana 47405*

[7]*Carleton University, Ottawa, Ontario, Canada K1S 5B6*

and the Institute of Particle Physics, Canada

[8]*University of Kansas, Lawrence, Kansas 66045*

[9] *Luther College, Decorah, Iowa 52101*

[10] *University of Minnesota, Minneapolis, Minnesota 55455*

[11] *Northwestern University, Evanston, Illinois 60208*

[12] *State University of New York at Albany, Albany, New York 12222*

[13] *Ohio State University, Columbus, Ohio 43210*

[14] *University of Oklahoma, Norman, Oklahoma 73019*

[15] *University of Pittsburgh, Pittsburgh, Pennsylvania 15260*

[16] *University of Puerto Rico, Mayaguez, Puerto Rico 00681*

[17] *Purdue University, West Lafayette, Indiana 47907*

[18] *Rensselaer Polytechnic Institute, Troy, New York 12180*

[19] *University of Rochester, Rochester, New York 14627*

[20] *Southern Methodist University, Dallas, Texas 75275*

[21] *Syracuse University, Syracuse, New York 13244*

[22] *Vanderbilt University, Nashville, Tennessee 37235*

[23] *Wayne State University, Detroit, Michigan 48202*

[24] *Carnegie Mellon University, Pittsburgh, Pennsylvania 15213*

(Dated: December 5, 2005)

We determine the di-electron widths of the $\Upsilon(1S)$, $\Upsilon(2S)$, and $\Upsilon(3S)$ resonances with sub-2% precision by integrating the cross-section of $e^+e^- \to \Upsilon$ over e^+e^- center-of-mass energy. Using energy scans at the Cornell Electron Storage Ring and measuring Υ production with the CLEO detector, we find di-electron widths of 1.252 $\pm$ 0.005 *(stat)* $\pm$ 0.019 *(syst)* keV, 0.581 $\pm$ 0.006 $\pm$ 0.009 keV, and 0.413 $\pm$ 0.004 $\pm$ 0.006 keV for the $\Upsilon(1S)$, $\Upsilon(2S)$, and $\Upsilon(3S)$, respectively.

PACS numbers: 14.40.Nd

The widths of the Υ meson, a $b\bar{b}$ bound state discovered in 1977 [1], are related to the quark-antiquark spatial wave function at the origin [2]. Recently, these widths have been recognized as a testing ground for QCD lattice gauge theory calculations [3]. Improvements in the lattice calculations, such as the avoidance of the quenched approximation [4], provide an incentive for more accurate experimental tests. The di-electron widths, Γ_{ee}, of the $\Upsilon(1S)$, $\Upsilon(2S)$, and $\Upsilon(3S)$ are currently measured to 2.2%, 4.2%, and 9.4% [5]. Validation of these lattice calculations at the few percent level will increase confidence in similar calculations used to extract important weak interaction parameters from data.

In particular, Γ_{ee} and f_D [6] are complimentary tests of the calculation of f_B, which is used to determine the CKM parameter V_{td}.

Our measurement of Γ_{ee} follows the method of [5]: we integrate the production cross section of Υ over incident e^+e^- energies. Then,

$$\Gamma_{ee} = \frac{{M_\Upsilon}^2}{6\pi^2} \int \sigma(e^+e^- \to \Upsilon)\, dE, \tag{1}$$

ignoring initial state radiation and beam energy spread. We also determine the Υ full widths using $\Gamma = \Gamma_{ee}/\mathcal{B}_{ee}$ where $\mathcal{B}_{ee}$ is the $\Upsilon \to e^+e^-$ branching fraction, and assume $\mathcal{B}_{ee} = \mathcal{B}_{\mu\mu}$ to take advantage of the well-measured $\Upsilon \to \mu^+\mu^-$ branching fractions [7].

The Cornell Electron Storage Ring (CESR), a symmetric e^+e^- collider, scanned center-of-mass energies in the vicinity of the $\Upsilon(1S)$, $\Upsilon(2S)$, and $\Upsilon(3S)$ and the CLEO-III detector collected the Υ decay products to determine the cross section at each energy. A fit to this resonance lineshape yields $\int \sigma(e^+e^- \to \Upsilon)\, dE$. This fit includes the effects of initial state radiation, beam energy spread, backgrounds, and interference between Υ and continuum final states. The eleven $\Upsilon(1S)$, six $\Upsilon(2S)$, and seven $\Upsilon(3S)$ scans have an integrated luminosity of 0.27, 0.08, and 0.22 fb^{-1}, with 0.19, 0.41, and 0.14 fb^{-1} of data below each peak to constrain backgrounds.

The CLEO-III detector is a nearly 4π tracking volume surrounded by a CsI crystal calorimeter [8]. Charged tracks are reconstructed in a 47-layer wire drift chamber and 4-layer silicon strip detector, and their momenta are inferred from their radii of curvature in a 1.5 T magnetic field. The calorimeter forms a cylindrical barrel around the tracking volume, reaching angles θ with respect to the beam axis of $|\cos\theta| < 0.85$, with endcaps extending this range to $|\cos\theta|$ < 0.98. Electron showers have a resolution of 75 MeV at beam energy (5 GeV).

The Υ mesons are produced nearly at rest and decay into leptonic final states e^+e^-, $\mu^+\mu^-$, or $\tau^+\tau^-$, or into approximately ten hadrons through strong decay via ggg or $gg\gamma$ intermediate states, or through electroweak decay via a $q\bar{q}$ intermediate state. The $\Upsilon(2S)$ and $\Upsilon(3S)$ can also make transitions into other $b\bar{b}$ resonances such as $\chi_{bJ}(nP)$, $\Upsilon(1S)$, and $\Upsilon(2S)$. The leptonic decays together account for only about 7% of the decays of each resonance and are difficult to distinguish from background, so we select hadrons, fit the hadronic cross section, and report $\Gamma_{ee}\Gamma_{\text{had}}/\Gamma_{\text{tot}}$. We then correct for the missing leptonic modes to report Γ_{ee}.

Bhabha scattering ($e^+e^- \to e^+e^-$) is our largest background. We suppress these events by requiring the greatest track momentum (P_{max}) to be less than 80% of the beam energy, shown in Figure 1-a, which reduces the Bhabha background to approximately the same magnitude as the hadronic continuum ($e^+e^- \to q\bar{q}$) background. Continuum

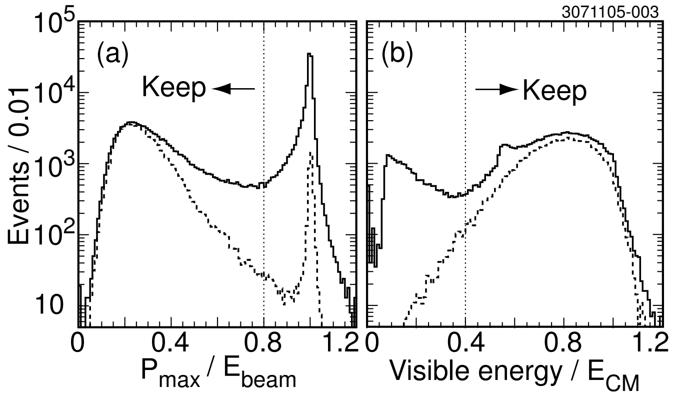

FIG. 1: Two of the distributions used to identify hadronic Υ decays. Solid histograms are data, dashed are simulated Υ decays, both with all hadronic selection criteria applied except the one shown.

annihilation processes such as these are accounted for by including a $1/s$ term in the lineshape fit, where $s = {E_{\mathrm{CM}}}^2 = (2E_{\mathrm{beam}})^2$.

Two-photon fusion events ($e^+e^- \to e^+e^-X$) contribute a non-$1/s$ background, so we suppress these by requiring the total visible energy (energy sum of all charged tracks and neutral showers) to be more than 40% of the center-of-mass energy, shown in Figure 1-b. A small $\log s$ term (8% of continuum below $\Upsilon(1S)$) and a $1/(\sqrt{s} - M_\Upsilon)$ term for each of the lighter Υ resonances (about 0.5% of continuum) are also added to the fit function. Because the off-resonance data points are only 20 MeV below each resonance, the different functional forms affect the background estimation at the peak by less than 0.04%.

Cosmic rays and beam-gas (collisions between a beam electron and a gas nucleus inside the beampipe) are suppressed by requiring charged tracks to point toward the collision point. We reduce this to less than 1% of the continuum by demanding that at least one reconstructed track pass within 5 mm of the beam axis and the vertex reconstructed from all primary tracks be within 7.5 cm of the collision point along the beam axis. We determine and subtract the remaining contamination at each energy using special single-beam and no-beam data runs normalized using events with a solitary large impact parameter track (for cosmic rays) or vertices along the beam axis but far from the collision point (for beam gas).

Backgrounds are summarized in Figure 2.

While our hadronic selection criteria eliminate essentially all $\Upsilon \to e^+e^-$ and $\Upsilon \to \mu^+\mu^-$ decays, they accept 57% of $\Upsilon \to \tau^+\tau^-$, according to a GEANT-based Monte Carlo simulation [9] including final state radiation [10]. We therefore

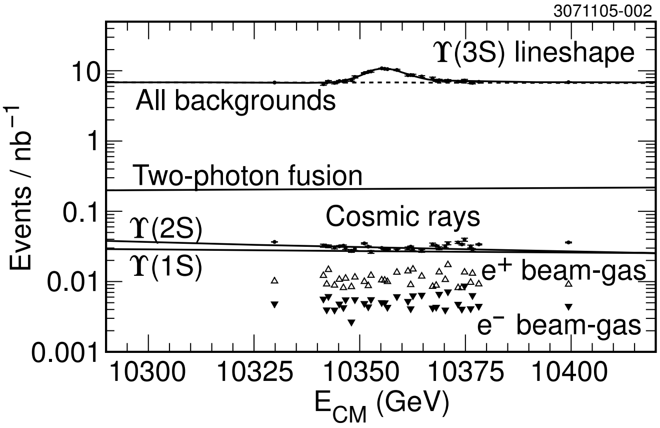

FIG. 2: The event yield as a function of center-of-mass energy in the region of the $\Upsilon(3S)$. The top points are data, with the fit superimposed, and the dashed curve represents the sum of all backgrounds. The lower points and lines show the individual non-1/s background contributions.

include in the fit function an $\Upsilon \to \tau^+\tau^-$ background term, including interference with continuum $e^+e^- \to \tau^+\tau^-$, using the measured $\mathcal{B}_{\tau\tau}$ [11].

A small fraction of hadronic Υ decays fail our event selection criteria. Instead of estimating this inefficiency with the Monte Carlo simulation, which would introduce dependence on the decay and hadronization models, as well as the detector simulation, we use a data-based approach. We select $\Upsilon(2S) \to \pi^+\pi^-\Upsilon(1S)$ to study $\Upsilon(1S)$ decays tagged by $\pi^+\pi^-$. If the $\pi^+\pi^-$ were sufficient to satisfy the trigger, the efficiency would be the ratio of $\Upsilon(1S)$ events satisfying our selection criteria (excluding the $\pi^+\pi^-$ tracks and showers) to all $\Upsilon(1S)$ events.

We can apply the above procedure directly using a 1.3 fb^{-1} sample at the $\Upsilon(2S)$ peak and a special two-track trigger, but this trigger is prescaled, so this procedure can only determine the hadronic efficiency to 3% of itself. Therefore, we use the two-track trigger to determine the efficiency of an unprescaled but more restrictive hadronic trigger ($\epsilon_{\rm htrig}$), and then use the full statistics from the hadronic trigger to determine our selection efficiency, once this trigger has been satisfied ($\epsilon_{\rm cuts}$). Our selection efficiency is then the product of $\epsilon_{\rm htrig}$ and $\epsilon_{\rm cuts}$.

The mass of the system recoiling against the $\pi^+\pi^-$ candidates in the two-track trigger sample is shown in Figure 3-a and the subset of events that fail the hadronic trigger is shown in Figure 3-b. After correcting for leptonic decays in the $\Upsilon(1S)$ sample, we find $\epsilon_{\rm htrig} = (99.59\ ^{+0.29}_{-0.45})\%$ from the ratio of fit yields.

From $\Upsilon(2S) \to \pi^+\pi^-\Upsilon(1S)$ events that satisfy the hadronic trigger, we find $\epsilon_{\rm cuts} = (98.33 \pm 0.33)\%$. This has been corrected for leptonic decays, the boost of the $\Upsilon(1S)$, track and shower confusion from the $\pi^+\pi^-$, and the efficiency

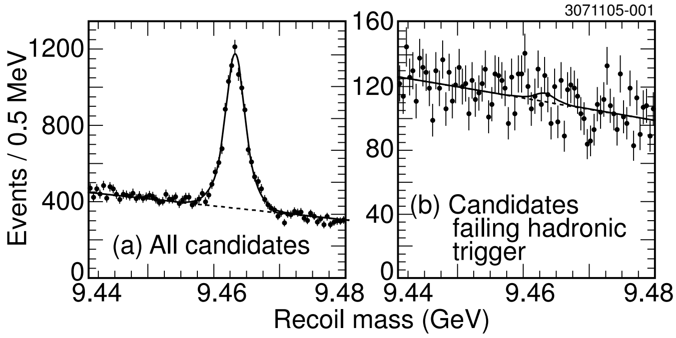

FIG. 3: Mass of the system recoiling against the $\pi^+\pi^-$ in $\Upsilon(2S) \to \pi^+\pi^-\Upsilon(1S)$ candidates satisfying the two-track trigger. The solid curve is a double Gaussian fit and the dashed curve is a linear background.

of the full set of triggers. Only the first correction is significant. Our event selection and trigger efficiency is therefore $(97.93\ ^{+0.44}_{-0.56})\%$ for the sum of all non-leptonic $\Upsilon(1S)$ decays.

To find the $\Upsilon(2S)$ and $\Upsilon(3S)$ efficiencies, we correct the $\Upsilon(1S)$ efficiency for energy dependence and for transitions specific to these excited states, using simulations. Only transitions to lower Υ resonances which then decay to e^+e^- or $\mu^+\mu^-$ introduce a significant correction. We measure the branching fractions of these $X\ell^+\ell^-$ decays to be $(1.58 \pm 0.16)\%$ and $(1.34 \pm 0.13)\%$, respectively, resulting in $\Upsilon(2S)$ and $\Upsilon(3S)$ efficiencies of $(96.18\ ^{+0.44}_{-0.56} \pm 0.15)\%$ and $(96.41\ ^{+0.44}_{-0.56} \pm 0.13)\%$, where the first uncertainty is common to all three resonances.

We use Bhabha events to determine the relative luminosity of each scan point. We select the Bhabhas by requiring two or more central tracks with momenta between 50% and 110% of the beam energy, and E/p consistent with e^+ and e^-. Contamination from $\Upsilon \to e^+e^-$ is 2–5% and is readily calculated given $\mathcal{B}_{\mu\mu}$ once we have done our Υ lineshape fit. Our subtraction includes energy-dependent interference between $\Upsilon \to e^+e^-$ and Bhabhas.

We determine the overall luminosity scale using the method of [12] from Bhabhas, $e^+e^- \to \mu^+\mu^-$, and $e^+e^- \to \gamma\gamma$, with the Babayaga event generator [13]. The systematic uncertainties from the three processes are 1.6%, 1.6%, and 1.8%, respectively, dominated by track finding and resonance interference for e^+e^- and $\mu^+\mu^-$, and by photon finding and angular resolution for $\gamma\gamma$. The three measurements give consistent results off-resonance, where Υ contamination is negligible. We use the weighted mean to determine the luminosity, and take the RMS scatter of 1.3% as the systematic uncertainty.

Bhabha and $\gamma\gamma$ luminosities, normalized to the same value off-resonance, deviate by $(0.8 \pm 0.2)\%$, $(0.3 \pm 0.4)\%$, and $(0.7 \pm 0.2)\%$ at the $\Upsilon(1S)$, $\Upsilon(2S)$, and $\Upsilon(3S)$ peaks. We correct each Γ_{ee} by half of its discrepancy and take half the discrepancy and its uncertainty in quadrature as a systematic uncertainty.

Accurate measurement of beam energy is also important for determining Γ_{ee}. An NMR probe calibrates the field of the CESR dipole magnets and hence provides the beam energy, after corrections for RF frequency shifts, steering and focusing magnets, and electrostatic electron-positron separators. To limit our sensitivity to drifts in this measurement, we limit scans to 48 hours and alternate measurements above and below the peak. By repeating a resonance cross-section measurement at a point of high slope, we find that beam energy calibration drifts by less than 0.04 MeV within each scan (68% C.L.), which implies a 0.2% uncertainty in Γ_{ee}.

The data for each resonance are separately fit to a lineshape function that consists of a three-fold convolution of (a) a Breit-Wigner resonance including interference between $\Upsilon \to q\bar{q}$ and $e^+e^- \to q\bar{q}$, (b) an initial state radiation distribution as given in Equation 28 of [14], and (c) the Gaussian spread in CESR beam energy, plus the background terms described above. The radiative corrections account for emission of real and virtual photons by the initial e^+e^-. We do not correct for vacuum polarization, which is absorbed into the definition of Γ_{ee}. The resulting Γ_{ee} values therefore should represent the Born diagram coupling a pure e^+e^- state to the Υ. The lineshape fits are insensitive to the Breit-Wigner widths, which are fixed to the PDG values [5]. The $\Upsilon(1S)$ lineshape is sensitive to the amount of hadronic interference, which would increase if Υ decays via ggg interfered with $q\bar{q}$ decays from the continuum. Assuming that $\Upsilon \to ggg$ and $\Upsilon \to q\bar{q}$ processes have no relative phase, the data disfavor such additional interference. The value of $\Gamma_{ee}\Gamma_{\rm had}/\Gamma_{\rm tot}$ of each resonance is allowed to float, as is the continuum normalization, and, to remove sensitivity to beam energy shifts between scans, the peak energy of each scan. In addition, we fit for the beam energy spread of groups of scans with common CESR horizontal steerings, but allow shifts when the steerings change, since they can change the beam energy spread by 1%. Uncertainties from radiative corrections, $\tau^+\tau^-$ normalization, and continuum interference add 0.2% to the uncertainty in $\Gamma_{ee}\Gamma_{\rm had}/\Gamma_{\rm tot}$.

The results are plotted in Figure 4. The fit function describes the data well, though the $\Upsilon(1S)$ and $\Upsilon(2S)$ have large χ^2 values. The χ^2 per degree of freedom ($N_{\rm dof}$) for $\Upsilon(1S)$ is 240/187 (0.5% confidence), for $\Upsilon(2S)$ is 107/66 (0.1% confidence), and for $\Upsilon(3S)$ is 155/159 (59% confidence). Pull distributions versus energy and versus date show no obvious trends, so we take the large χ^2 values as an indication that point-by-point uncertainties are underestimated, and increase the statistical uncertainty by $\sqrt{\chi^2/N_{\rm dof}}$ if it is greater than unity.

All uncertainties are listed in Table I.

Our values of $\Gamma_{ee}\Gamma_{\rm had}/\Gamma_{\rm tot}$, listed in Table II, are consistent with, but more precise than, but PDG world averages [5] and our $\Upsilon(3S)$ measurement is substantially more precise than the previous one. To determine Γ_{ee} for each

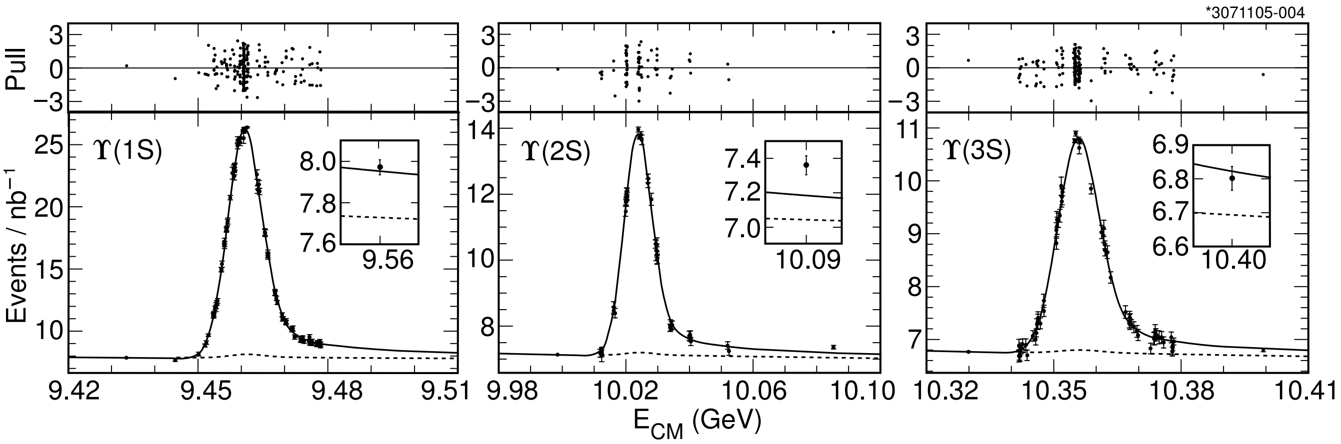

FIG. 4: The hadronic yield versus center-of-mass energy in the vicinity of the three Υ resonances. Points are data, corrected for fitted beam energy shifts between scans, the solid line is the fit, the dashed line is sum of all backgrounds, and the insets show high-energy measurements. Above each fit is the pull distribution (residual divided by uncertainty).

resonance, also listed in the Table, we assume $\mathcal{B}_{ee} = \mathcal{B}_{\mu\mu} = \mathcal{B}_{\tau\tau}$ and obtain $\mathcal{B}_{\mu\mu}$ from [7]. Also assuming $\mathcal{B}_{ee} = \mathcal{B}_{\mu\mu}$, we obtain new values of the Υ full widths: 54.4 $\pm$ 0.2 *(stat)* $\pm$ 0.8 *(syst)* $\pm$ 1.6 *($\mathcal{B}_{\mu\mu}$)* keV, 30.5 $\pm$ 0.3 $\pm$ 0.5 $\pm$ 1.3 keV, and 18.6 $\pm$ 0.2 $\pm$ 0.3 $\pm$ 0.9 keV.

We gratefully acknowledge the effort of the CESR staff in providing us with excellent luminosity and running conditions. This work was supported by the A.P. Sloan Foundation, the National Science Foundation, and the U.S. Department of Energy.

[1] S. W. Herb *et al.*, Phys. Rev. Lett. **39**, 252 (1977).

[2] R. Van Royen and V. F. Weisskopf, Nuovo Cim. A **50**, 617 (1967) [Erratum-ibid. A **51**, 583 (1967)].

[3] A. Gray, I. Allison, C. T. H. Davies, E. Gulez, G. P. Lepage, J. Shigemitsu and M. Wingate, arXiv:hep-lat/0507013.

[4] C. T. H. Davies *et al.* [HPQCD Collaboration], Phys. Rev. Lett. **92**, 022001 (2004) [arXiv:hep-lat/0304004].

[5] S. Eidelman *et al.* [Particle Data Group], Phys. Lett. B **592**, 1 (2004).

[6] M. Artuso *et al.* [CLEO Collaboration], arXiv:hep-ex/0508057.

[7] G. S. Adams *et al.* [CLEO Collaboration], Phys. Rev. Lett. **94**, 012001 (2005).

[8] G. Viehhauser *CLEO III Operation*, Nucl. Instrum. Methods A **462**, 146 (2001).

[9] R. Brun *et al.*, Geant 3.21, CERN Program Library Long Writeup W5013 (1993), unpublished.

[10] E. Barberio and Z. Wąs, Comput. Phys. Commun. **79**, 291 (1994).

TABLE I: All uncertainties in Γ_{ee} in the order in which they are discussed in the text. Uncertainties common to all resonances are indicated with an asterisk ($*$). Statistical uncertainty is multiplied by the $\sqrt{\chi^2/N_{\rm dof}}$ of the fit (see text).

Contribution to Γ_{ee}	$\Upsilon(1S)$	$\Upsilon(2S)$	$\Upsilon(3S)$
Correction for leptonic modes	0.2%	0.2%	0.3%
*Hadronic efficiency	0.5%	0.5%	0.5%
Xe^+e^-, $X\mu^+\mu^-$ correction	0	0.15%	0.13%
*Overall luminosity scale	1.3%	1.3%	1.3%
Bhabha/$\gamma\gamma$ inconsistency	0.4%	0.4%	0.4%
Beam energy measurement drift	0.2%	0.2%	0.2%
Fit function shape	0.2%	0.2%	0.2%
Total systematic uncertainty	1.5%	1.5%	1.5%
Scaled statistical uncertainty	1.1×0.3%	1.3×0.7%	1.0%
Total	1.5%	1.7%	1.8%

TABLE II: The results of $\Gamma_{ee}\Gamma_{\rm had}/\Gamma_{\rm tot}$ for the three resonances, the di-electron widths Γ_{ee}, and their ratios. The first uncertainty is scaled statistical and the second is systematic.

$\Gamma_{ee}\Gamma_{\rm had}/\Gamma_{\rm tot}(1S)$	$(1.252 \pm 0.004 \pm 0.019)$ keV
$\Gamma_{ee}\Gamma_{\rm had}/\Gamma_{\rm tot}(2S)$	$(0.581 \pm 0.005 \pm 0.009)$ keV
$\Gamma_{ee}\Gamma_{\rm had}/\Gamma_{\rm tot}(3S)$	$(0.413 \pm 0.004 \pm 0.006)$ keV
$\Gamma_{ee}(1S)$	$(1.354 \pm 0.005 \pm 0.020)$ keV
$\Gamma_{ee}(2S)$	$(0.619 \pm 0.006 \pm 0.009)$ keV
$\Gamma_{ee}(3S)$	$(0.446 \pm 0.004 \pm 0.007)$ keV
$\Gamma_{ee}(2S)/\Gamma_{ee}(1S)$	$(0.457 \pm 0.004 \pm 0.003)$
$\Gamma_{ee}(3S)/\Gamma_{ee}(1S)$	$(0.329 \pm 0.003 \pm 0.002)$
$\Gamma_{ee}(3S)/\Gamma_{ee}(2S)$	$(0.720 \pm 0.010 \pm 0.006)$

[11] `http://www.lip.pt/events/2005/hep2005/talks/ hep2005_talk_JeanDuboscq.pdf`, pages 14–18.

[12] G.D. Crawford *et al.* (CLEO Collaboration), Nucl. Instrum. Methods Phys. Res., Sect A **345**, 429 (1994).

[13] C.M. Carloni Calame *et al.*, Nucl. Phys. Proc. Suppl. B **131**, 48 (2004).

[14] E. A. Kuraev and V. S. Fadin, Sov. J. Nucl. Phys. **41**, 466 (1985) [Yad. Fiz. **41**, 733 (1985)].